A Kinematics-Based Simulation Framework for Face Gear Hobbing and Manufacturing Error Analysis

Ali Bilen[1*], Nikolas Paul Braunschweiger[1], Rijad Karabegović[1], Tobias Felix Kircher[1], Francisco Eduardo Waggershauser[1], Philipp Malte Wübbena[1], Nitish Kumar[1], Larissa Antonia Weiland[1], Linus Robert Reister[1], Edouard Gindin[3], Prof. Dr.-Ing. Gisela Lanza[1,2]

[1]Karlsruhe Institute of Technology (KIT), Institute of Production Science (wbk), Karlsruhe, Germany

[2]Global Advanced Manufacturing Institute (GAMI),
Suzhou SILU Production Engineering Services Co., Ltd., Suzhou, P. R. China

[3]FRENCO GmbH, Altdorf, Germany

E-mail: *ali.bilen@kit.edu

Abstract

Face gears are increasingly used in compact precision assemblies, yet systematic knowledge about how manufacturing errors propagate into functional deviations remains limited. In particular, the kinematics of the hobbing process for face gears differs fundamentally from established processes for cylindrical gears, resulting in complex sensitivity patterns with respect to tool positioning, machine errors, and process parameter variations. This paper presents a kinematics-based simulation framework to analyze the influence of characteristic error sources in the hobbing process on the resulting crown-gear geometry. The approach models the full engagement between the virtual hob and workpiece and allows the systematic introduction of geometric and kinematic deviations, such as tool runout, axial and radial misalignments, pitch errors, and spindle-related perturbations. The resulting gear topographies are evaluated with geometry-based metrics relevant for micro-scale applications to characterize their impact on flank shape, symmetry, and tooth-space formation. The results provide qualitative insights into which error mechanisms most strongly affect the geometric features of face gears and under which conditions these sensitivities become critical.

1 Introduction

Face gears (also referred to as face gears) represent a key class of mechanical components used in compact transmission systems, precision instruments, and micro-mechanical assemblies [12]. Their capability to transmit motion between non-parallel axes - combined with a high degree of functional robustness - makes them attractive for applications in which installation space, efficiency, and reliability are critical [16]. However, as manufacturing scales toward micro-geometries, ensuring high precision becomes increasingly demanding. Reduced module sizes amplify the influence of process fluctuations, while conventional metrology approaches face fundamental limitations concerning sensor accessibility, resolution, and measurement stability [18, 4].

A central challenge arises from the limited understanding of how specific deviations during manufacturing propagate into geometric and functional errors on the finished gear. In contrast to involute cylindrical gears, where standardized evaluation procedures exist, face gears lack comparably established inspection routines and interpretation methods [17]. Experimental investigations alone are therefore insufficient to capture the full parameter sensitivity, particularly when isolated error sources must be introduced in a controlled manner.

Kinematic simulation offers a promising solution to this gap. By virtually reproducing the engagement between tool and workpiece, gear-generation models allow individual process parameters—such as translational offsets ($\Delta x, \Delta y, \Delta z$), angular misalignments, tool runout, or kinematic imbalance—to be varied independently. This enables systematic error studies that cannot be cleanly reproduced on a physical machine.

Against this background, the present work develops a kinematics-based simulation framework for the hobbing of face gears that serves two complementary purposes:

1. **Generation of parametrized nominal geometries**: A spur-gear-based virtual tool model is used to generate idealized face gear geometries. The target geometry is thus defined purely through the parameters of the generating spur gear and the prescribed rolling kinematics.

2. **Analysis of error–effect relationships**: By introducing deviations into selected model parameters, the framework enables a systematic investigation of how individual and combined error sources manifest on the resulting tooth geometry.

In summary, the contribution of this work is a unified simulation approach that provides both (i) a parametrizable source of reference geometries for benchmarking and metrology validation, and (ii) a diagnostic instrument to trace quality-critical deviations back to their causes in manufacturing. These advances form the basis for future compensation strategies and support the long-term objective of simulation-based quality assurance in the production of face and micro-face gears.

2 Fundamentals

This section presents the fundamental geometric properties of face gears and gear hobbing as a manufacturing process as well as the tools used for this purpose.

2.1 Geometry of Face Gears

Involute gears represent the industrial standard for power transmission due to their favorable kinematic properties [8], including a straight line of action and robustness with respect to center distance variations [2]. By contrast, the tooth geometry of face gears (depicted in 1) is **non-involute** [16]. The tooth flanks of a face gear do not result from the involute construction on a base circle, but emerge as the *generating surface* produced by the rolling motion of the mating spur gear. Accordingly, the flank can be interpreted as a contact trace or kinematic envelope rather than a pure involute [16].

From a mathematical perspective, the resulting flank can also be described as the geometry generated by a spatial rotation of the pinion's involute profile, which sweeps out the three-dimensional tooth surface during the meshing motion. Litvin characterizes this surface as a kinematically generated envelope derived from the rotated involute, rather than an analytically closed involute surface on the face gear itself [10].

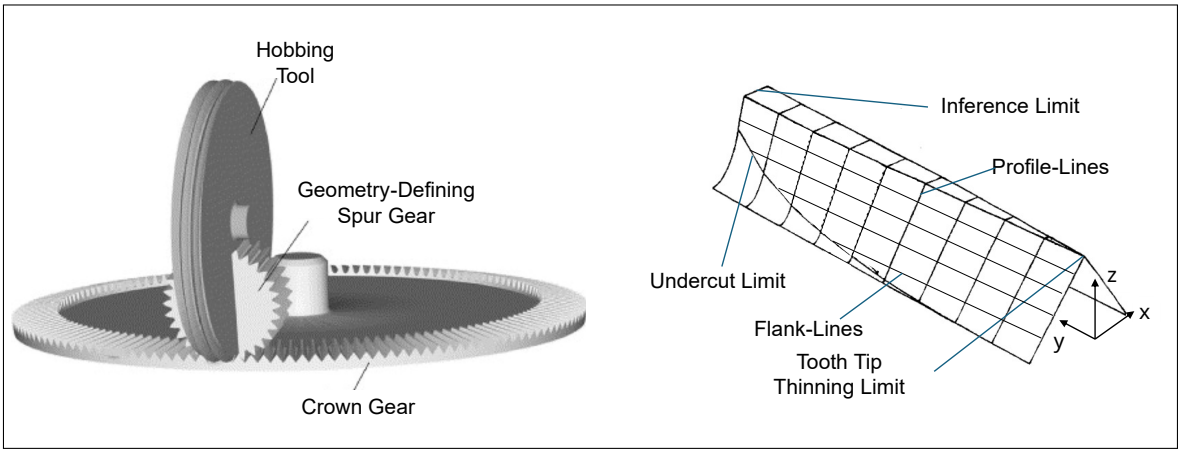

Figure 1: Manufacturing of face gears on the left [13], Geometry of resulting tooth on the right, based on [11]

Face gears can be considered as bevel gears with a pitch cone angle of $\delta = 90°$ meshing with a cylindrical spur pinion [16]. A key characteristic of this configuration is the axial freedom of the pinion, such that axial positioning errors do not affect the transmission ratio or the fundamental meshing conditions [16]. This property makes face gears particularly attractive for compact and misalignment-tolerant drive systems.

In contrast to spur gears with constant geometry along the face width, face gears exhibit a continuously varying pressure angle α as a function of the radial position, governed by

$$d \cdot \cos\alpha = \text{const.} \tag{1}$$

This variation introduces inherent geometric limits that restrict the usable face width. At small radii, undercutting may occur due to excessively small pressure angles, whereas at large radii tooth pointing can arise [7]. Furthermore, comprehensive standards defining tolerance classes for face gears are currently not available, which complicates both manufacturing and quality assessment.

Geometric deviations are commonly described with respect to three principal directions: tooth profile, flank line, and pitch [8]. For face gears, the tooth profile is defined in normal sections

through the tooth height, while the flank line describes the geometry along the face width. Due to the inherently three-dimensional tooth geometry and the radial variation of the pressure angle, deviations along the face width cannot be evaluated independently of the radial position. The tooth flanks are generated as the envelope of the cutting tool, resulting in a conjugate gear pair [13]. Depending on the axial position of the cutting pinion, symmetric or asymmetric flank geometries may arise [16].

Figure 1 illustrates the definition of profile and flank directions for face gears and serves as a geometric reference for the subsequent modeling and simulation of the hobbing process.

2.2 Hobbing for Face Gear Manufacturing

The following paragraph explains the development of the tools used to manufacture face gears and the underlying manufacturing process.

Face gears can be manufactured using broaching, gear shaping and gear hobbing among other methods [16]. Gear hobbing, which will be examined here, is a continuous method for machining gears that is also used in face gear production [8]. The used hobbing tools must have a profile that corresponds exactly to it's mating gear, an involute spur gear [20]. To theoretically derive the hob from a spur gear, a basic worm is created from the tooth profile of the spur gear. This relationship can be representet by the so-called "virtual shaper" (visualized in Fig. 2), a spur gear whose profile exactly matches the profile of the hob [19]. This results in thread-shaped cutting lugs [16]. As a result of this condition, a tool is created that continuously corresponds to the tooth profile of the underlying spur gear. A rotational movement of this tool around its own axis of rotation would therefore correspond to a rolling movement of the spur gear on the face gears gear [20], which corresponds to the requirement formulated in [4]. In terms of tool geometry, a distinction is made between barrel-shaped, spherical, and torus-shaped tools, which is shown in Figure 2 [16]. In practice, toroidal hobs are typically preferred for face gear manufacturing due to their favorable generating geometry.

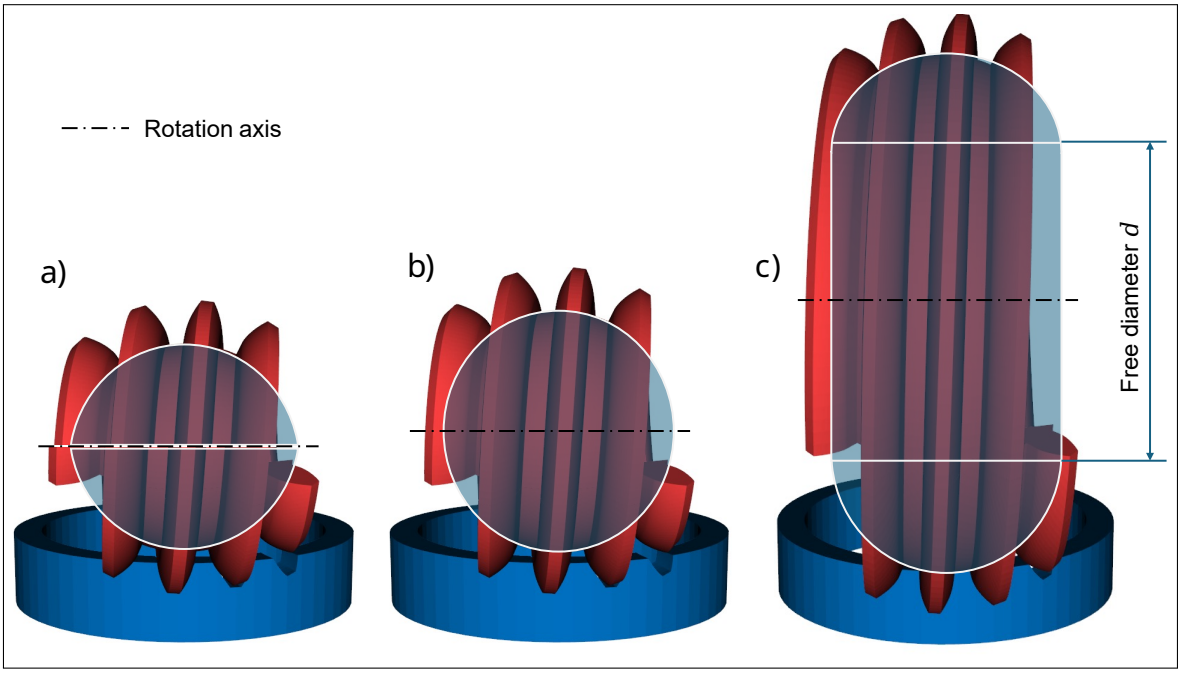

Figure 2: Types of tool geometries, showing a barrel-shaped (a), sperical (b) and torus-shaped tool (c) from left to right. Inspired by [16].

Face gears are manufactured using the tool by rotating the tool around its own axis and simultaneously rotating the body of the face gear around its own axis [19]. This replicates the movement of a spur gear along the face gears face. During this process, the tool and face gear are at an constant cone angle δ of 90° to each other [19], in order to produce the characteristic shape of the face gear as defined in [16]. This arrangement means that the tool always corresponds to a tooth profile of the spur gear that defines the face gears wheel, but removes material at the same time by rotating around its own axis. In a kinematic way, rotating a spur gear along the face gears face and using gear hobbing on a face gear is equivalent. The rotation ratio between the face gear and the tool is described by the fraction N_W/N_1, where N_W corresponds to the number of threads of the tool

and N_1 corresponds to the number of teeth of the resulting face gear [19, 20]. In addition to the rotational movement of the two bodies, the tool must also undergo an radial feed movement in order to produce the geometry of the face gears wheel [19].

3 State of the Art

The generation, manufacturing, and inspection of face gears (also crown gears) requires the coordinated interplay of geometric modeling, simulation, and metrology. This becomes particularly critical in micro-scale applications, where scaling effects amplify even minor deviations and conventional tolerancing concepts reach their limits. Current research therefore spans three primary domains: (i) deviation-oriented metrology, (ii) mathematical representation of tooth flank geometry, and (iii) software-supported generation and simulation. Although each field has matured individually, their integration into a unified framework for deriving nominal geometries *and* tracing manufacturing errors to geometric effects remains incomplete.

3.1 Metrology and Deviation Analysis

Physical measurements form the empirical foundation for quantifying geometric deviations between manufactured and nominal face gear geometries. Approaches by [14, 15, 17, 9] rely on tactile Coordinate Measurement Machines (CMMs) or high-resolution optical scanning to capture dense point clouds of entire tooth flanks. These data enable detailed assessment of profile, pitch, and surface deviations and thus provide a comprehensive view of the manufactured geometry. Optical systems in particular have become widely adopted due to their full-field measurement capability and high acquisition speed (see Fig. 3).

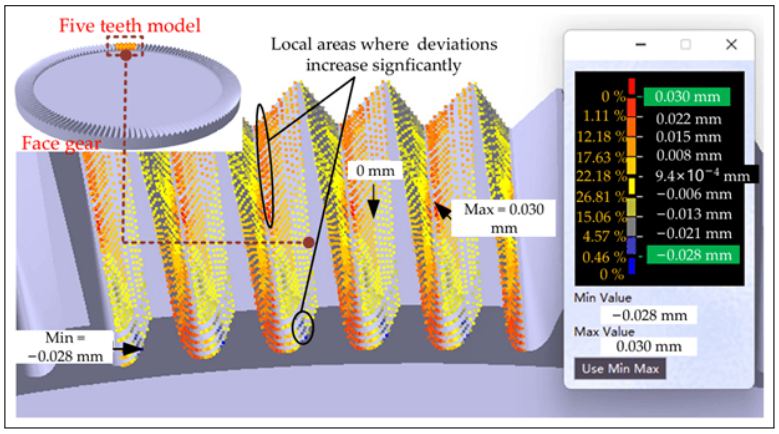

Figure 3: Comprehensive tooth flank deviation approach by [14].

However, optical systems are increasingly affected by reflections, shadowing, and limited accessibility in micro-geometries. Compensation concepts such as MOOM-CCME [15] and MECM [17] improve data quality, yet they remain diagnostic in nature: they quantify *what* deviation occurred, but cannot systematically infer *why* it occurred. In other words, they lack a causal link to specific process parameters such as axis offsets, spindle tilt, or tool runout—an aspect that becomes decisive when setup errors drastically scale in micro-face gears [9].

3.2 Nominal Geometry Generation and Software Tools

A second line of research concerns the derivation of nominal geometries used as reference surfaces for quality evaluation. In industrial practice, tools such as KISSsoft provide accessible design workflows, but rely on approximations that restrict exact flank representation for complex face gears [7]. FlaGen [6] expands this capability but remains oriented toward base data generation rather than metrological reference surfaces for systematic deviation analysis.

More advanced software solutions such as HyGEARS and ESCO's *eSkiving.FS* introduce kinematic simulation of cutting processes [5, 3]. These tools can generate high-quality nominal geometries but are primarily designed as forward models: their output depends on given parameters, yet they offer no systematic mechanism to vary parameters purposefully and study the geometric consequences in isolation. As a result, they generate usable nominal data, but do not function as analytical instruments for causality and process traceability. In practice, they therefore provide convenient solutions for obtaining face gear geometries, but they are not truly suitable for simulating the manufacturing

process itself, as they do not model the underlying process physics, parameter interactions, or error propagation in a way that supports targeted analysis.

3.3 Mathematical Representations and Envelope Theory

Theoretical modeling has advanced from virtual rack concepts to formulations grounded in differential geometry and envelope theory. Classical rack-based formulations introduce simplifications that limit the accurate representation of curved undercut regions and variable contact conditions [4]. Envelope theory, as formalized by Litvin [13], defines the flank surface as the envelope of the tool under relative motion:

$$\mathbf{n}(\mathbf{r}) \cdot \mathbf{v}_{12}(\mathbf{r}) = 0, \tag{2}$$

with $\mathbf{n}(\mathbf{r})$ denoting the surface normal and $\mathbf{v}_{12}(\mathbf{r})$ the relative velocity between tool and workpiece. Refined models by [6, 4] improve flank fidelity, in particular near undercut boundaries. However, these formulations have not yet been embedded into frameworks that enable sensitivity studies or inverse identification of setup errors.

3.4 Identified Research Gap

Across the reviewed literature, two structural limitations persist:

1. **Nominal geometries are generated, but not parametrically linked to a process model.** Existing tools create target surfaces but do not expose the underlying generating geometry as a controllable parameter space (e.g., spur-gear parameters, offsets, tilts).
2. **Simulation models are forward-oriented and do not support error–cause–effect analysis.** Deviations can be measured with high spatial resolution, but cannot yet be traced back to the machine settings that produced them.

This disconnect prevents the establishment of a closed methodological chain in which the same model can be used to (i) derive nominal geometries for quality assurance and (ii) introduce controlled deviations to study how individual parameters propagate into measurable geometric fingerprints.

3.5 Motivation for the Present Work

Against this background, the present work closes the identified gap by developing a kinematically driven simulation framework that serves a dual purpose. First, it generates parametrized nominal geometries based on a spur-gear tool model whose geometry directly defines the resulting face gear. Second, it enables systematic variation of machine parameters—such as translational offsets, angular misalignments, or runout—to analyze their geometric effects along the tooth flank. This duality forms the methodological foundation for simulation-supported quality assurance and root-cause-oriented deviation interpretation in micro-face gear manufacturing.

4 Approach

This work proposes a simulation-based approach for the systematic analysis of error–cause–effect relationships in the manufacturing of face gears. The core idea is to progressively increase the physical and process-related fidelity of the geometric modeling in order to balance computational efficiency with explanatory power. The approach starts with a spur-gear-based Boolean simulation to generate nominal face gear geometries and to investigate fundamental kinematic effects. While this abstraction is sufficient for analyzing basic geometric characteristics, it is not adequate for the investigation of specific manufacturing-related error sources. Therefore, the model is extended by an explicit, tool-based representation of the cutting process. In contrast to purely analytical formulations, a pragmatic, programmatic modeling strategy is pursued, enabling flexible integration of tool geometry, feed motion, and angular corrections resulting from tool helix and process kinematics. Based on this enhanced process model, a structured design of experiments is conducted to systematically vary machine and process parameters. The resulting geometric deviations are evaluated to identify sensitivities and to derive targeted correction strategies for manufacturing errors.

4.1 Reference Coordinate System and Symbols

The simulation is performed in a gear-fixed Cartesian coordinate system. The y-axis coincides with the tooth axis of the face gear, while the x-axis is oriented perpendicular to the tooth axis within the plane of the gear. Consequently, the x–y plane represents the planar reference surface of the face gear. The z-axis is oriented normal to this plane and corresponds to the axial direction of the

gear. This coordinate system serves as the common reference frame for all geometric evaluations and feature definitions used in this work. For clarity and consistency, all symbols and variables introduced in the following sections are summarized in a dedicated list of symbols.

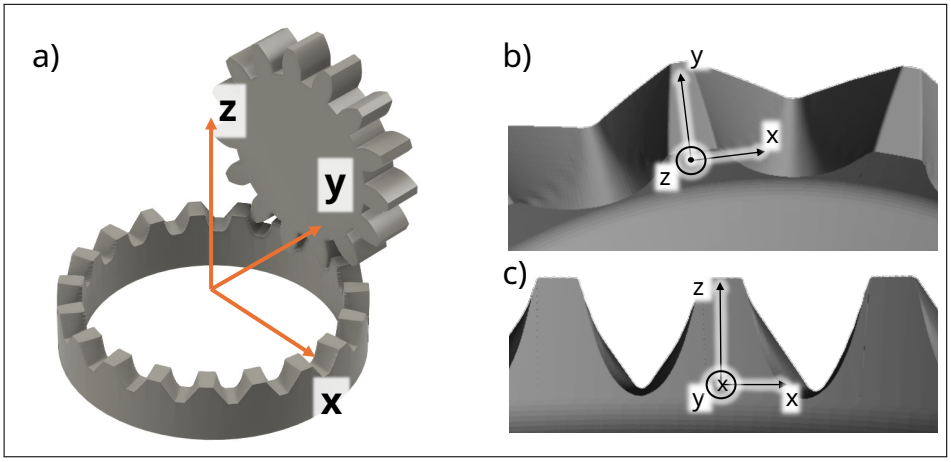

Figure 4: Coordinate System [4], a) visualizes the global position, b) shows an individuel tooth

List of Symbols

Symbol	Description
α	Tumble angle describing dynamic spindle/tool tilt
$\alpha(\varphi)$	Local helix angle of the wrapped spur-gear profile as a function of tool path position φ
α_{mean}	Mean effective helix angle used for tool orientation correction
d	Tumble distance; offset between ideal and actual spindle/tool rotation axis
$\Delta\theta$	Incremental angular rotation step per simulation iteration
$\Delta\vec{r} = (\Delta x, \Delta y, \Delta z)$	Vector of translational positioning deviations of the tool
Δx	Tangential positioning error (dominant source of flank asymmetry)
Δy	Radial positioning error (minor influence; no significant flank formation change)
Δz	Axial positioning error affecting tooth height and top-land geometry
$FaceGear_i$	Intermediate face-gear volume after simulation step i
i	Discrete simulation step index
L	Arc length of one complete profile winding on the toroidal tool path
N	Number of teeth of the generating (virtual) spur gear
p_t	Transverse pitch of the spur-gear profile
$\vec{p}_i = (x_i, y_i, z_i)$	Cartesian coordinate of the profile point at angular position φ_i
r_F	Radius of the circular tool path (toroidal tool radius)
$\vec{r}_{\text{nominal}}$	Nominal tool position vector
$\vec{r}_{\text{real}}$	Real tool position vector including translational deviations
ρ_i	Circumferential rotation applied to maintain pitch spacing at position φ_i
$\setminus$	Boolean difference operator for volumetric material removal
$SpurGear_i$	Instantaneous spur-gear volume acting as cutting tool at step i
t	Tumble amplitude (dynamic radial runout per revolution)
θ	Angular pitch of the spur gear, $\theta = 2\pi/N$
θ_{face}	Rotation angle of the face gear in the kinematic rolling process
θ_{spur}	Rotation angle of the spur-gear tool
φ_i	Angular position index along the tool path
Z_{face}	Tooth count of the resulting face gear
Z_{spur}	Tooth count of the generating spur gear

4.2 Model parameterization

The parameterization of the simulation follows a hierarchical structure in which the *generating spur gear* defines the geometry of the hobbing tool, and the tool in turn defines the emerging face gear geometry. Consequently, the spur gear parameters are the primary drivers of the resulting tooth shape, while simulation parameters mainly affect the runtime and numerical resolution, but not the nominal geometry itself.

Generating spur gear (primary geometry driver) The involute spur gear parametrizes the tooth profile that is mapped onto the toroidal tool and ultimately imprinted onto the face gear. The following parameters directly control the resulting face gear geometry:

- `module` m — scales tooth size and affects the resulting flank curvature.
- `teeth_spur` z_{spur} — defines circumferential spacing and tool pitch.
- `pressure_angle` α — influences the effective contact geometry.
- `profile_shift_factor` x — adjusts tooth thickness and prevents undercutting.
- `spur_gear_width` — controls the axial cutting range of the tool.

These parameters define the involute profile from which the tool is constructed, making them the highest-leverage input for geometry variation.

Tool construction (geometry transfer) The spur gear profile is wrapped along a toroidal path to form the cutting tool. Its size and discretization influence the fidelity of the cutter but do not redefine the tooth profile:

- `tool_radius`, `tool_width` — define the torus geometry.
- `tool_steps` — number of discretized profiles; higher values increase accuracy at the cost of longer computation time.

Face gear (workpiece) The workpiece description is minimal; it only scales and positions the generated geometry:

- `teeth_face` — resulting number of teeth.
- inner/outer diameter — define blank size and usable flank width.

Simulation parameters (runtime & resolution) These parameters affect numerical effort, Boolean robustness, and runtime — but not the underlying nominal geometry:

- `steps`, `tool_angle_step` — resolution of the rolling motion.
- `infeed_step` — incremental penetration; affects runtime and mesh load.
- `mesh_cleanup_interval` — maintains Boolean stability; higher values increase speed.

Manufacturing deviations (error introduction) Deviation parameters override the ideal kinematics and are used to reproduce characteristic manufacturing errors:

- static: $\Delta x, \Delta y, \Delta z$ (tool misalignment)
- dynamic: wobble angle α, wobble distance d (spindle/runout effects)

4.3 Spur-Gear-Based Boolean Simulation

In a first step, the simplest possible generative model is developed in order to establish a baseline for face gear geometry formation. Instead of modelling a dedicated hobbing cutter, the tool is deliberately substituted by a parametrized spur gear that directly interacts with the workpiece volume (see 5). Conceptually, this corresponds to a virtual cutter with an infinitely large tool diameter, such that the generating geometry is defined solely by the involute spur gear profile and the prescribed rolling motion. This abstraction allows the face gear geometry to be generated by purely geometric means via Boolean subtraction, without requiring a physical tool model.

Even at this level of abstraction, a wide range of effects can already be investigated: (i) translational misalignment in the x-, y-, and z-directions, (ii) the influence of tangential shifts on flank symmetry, (iii) penetration depth effects on tooth height and top-land geometry, and (iv) qualitative spindle-related disturbances such as wobble or runout. Thus, the model provides a first capability for studying how kinematic errors manifest as geometric artifacts on the resulting tooth flanks.

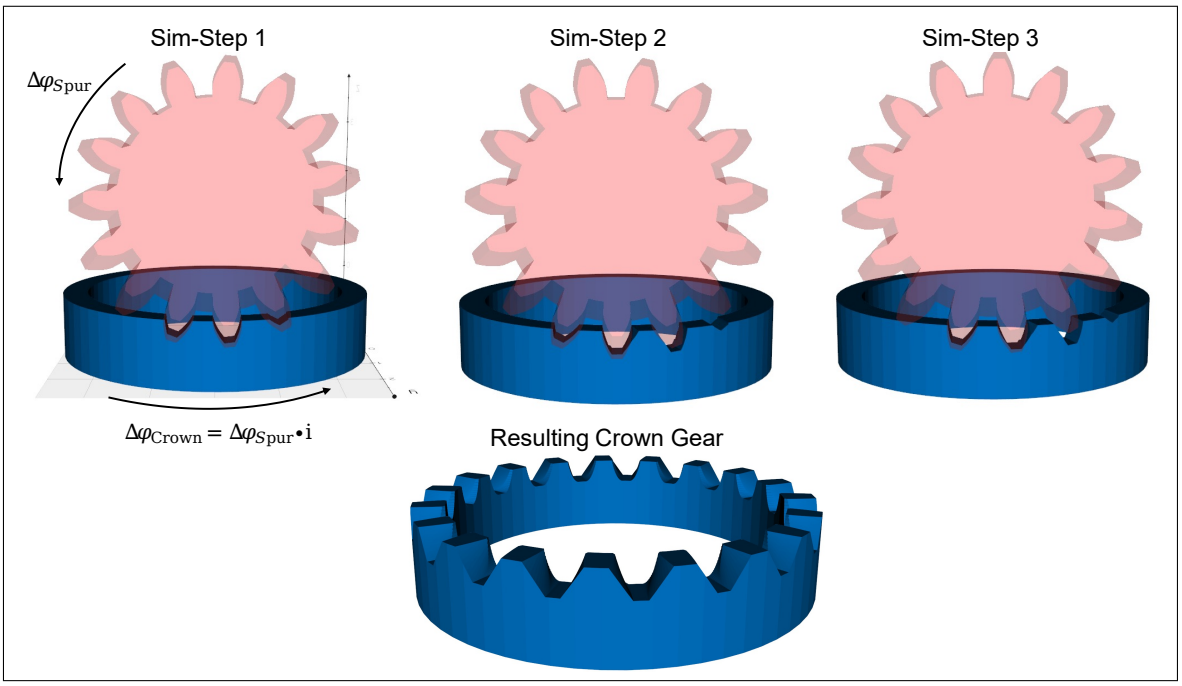

Figure 5: Spur-gear-based boolean simulation of face gear generation.

However, this simplified representation inherently omits tool-specific influences, such as geometry-induced helix effects, cutter edge kinematics, and the interaction between tool path and profile winding. These effects cannot be captured without an explicit tool model. For this reason, the subsequent step introduces a dedicated representation of the hobbing cutter, enabling the analysis of tool-induced deviations and the transition from an abstract generative model to a process-oriented simulation framework.

4.3.1 Assumptions and Boundary Conditions For the simulation, a fully parametrizable spur gear model is generated. Its geometry is generally described by the pressure angle, profile shift, addendum and dedendum diameters, and the number of teeth. This spur gear serves as a virtual tool. The rolling motion is defined along a fixed cylindrical surface, while the relative position between the spur gear and the cylinder is described by translational and rotational degrees of freedom. The simulation is restricted to the geometric interaction between tool and workpiece; physical effects such as forces, elastic deformations, or thermal influences are not considered.

4.3.2 Kinematic Modeling The motion of both bodies is described by their incrementally continued rotation. In each simulation step i, the spur gear rotates about its own axis, with the current rotation angle given by

$$\theta_{\text{spur}} = i \cdot \Delta\theta. \tag{3}$$

At the same time, the face gear is rotated by a proportional angle corresponding to the kinematic relationship of a real rolling process. Using the transmission ratio, the rotation angle of the face gear is given by

$$\theta_{\text{face}} = \theta_{\text{spur}} \cdot \frac{Z_{\text{spur}}}{Z_{\text{face}}}. \tag{4}$$

Since the axes of the spur gear and the face gear are orthogonal to each other, the spur gear rotates about its local y-axis, while the face gear rotates about its z-axis. Together with the translational positioning of the spur gear along the Cartesian axes, this results in a uniquely defined relative configuration of both bodies at each simulation step, which forms the basis for the subsequent geometric interaction.

The generation of the face gear geometry is then performed via incremental volumetric subtraction. For each time step i, the instantaneous volume of the spur gear is subtracted from the current workpiece volume. The geometric evolution can thus be expressed recursively as

$$\text{FaceGear}_{i+1} = \text{FaceGear}_i \setminus \text{SpurGear}_i, \tag{5}$$

where $\setminus$ denotes the applied boolean difference operation. After completing the rolling process, an idealized face gear geometry is obtained that is generated exclusively by geometric means.

4.4 Tool model

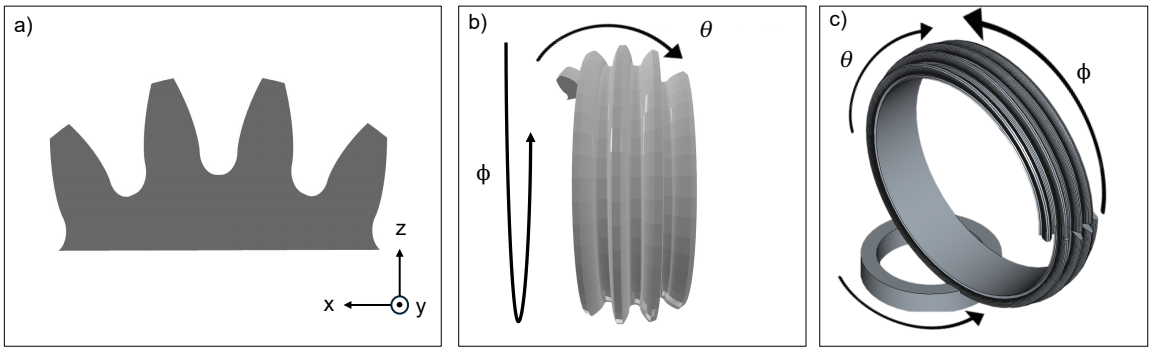

Figure 6: (a) Four-tooth involute profile in the normal section. (b) Mapping of the profile along the circular tool path. (c) Resulting three-dimensional tool geometry with helical cutting edges.

The objective of the tool model is to provide a geometrically consistent and kinematically generative representation of a face gear hobbing tool that is suitable for Boolean material removal simulations. In contrast to spur-gear-based Boolean approaches that directly impose a target tooth geometry, the proposed model derives the effective cutting geometry solely from the relative motion between tool and workpiece. This enables a causal investigation of how process kinematics and tool-related deviations affect the resulting face gear geometry.

The tool is modeled as a rigid, torus-based hobbing cutter whose functional cutting region is generated from a parametrically defined involute spur-gear profile. Tool wear, elastic deformations, cutting forces, and thermal effects are intentionally neglected in order to isolate the geometric consequences of the kinematic process.

Geometrically, the tool model is constructed in two stages:

1. **Profile generation in the normal section.** The starting point is an involute spur-gear tooth profile defined by the module, pressure angle, profile shift, and addendum and dedendum heights. The involute flank geometry is computed parametrically from the base circle radius. From a single tooth including the tooth gap, a closed four-tooth profile is generated by fourfold rotation with respect to the angular pitch $\theta = 2\pi/N$. The resulting contour is represented as a closed wire in the local tool coordinate system (Fig. 6a).

2. **Kinematic mapping onto the tool path.** The four-tooth profile is swept along a circular path of radius r_F in the xz-plane. For each discrete angular position φ_i along the path, the

profile undergoes a sequence of transformations that reflects the kinematics of the hobbing process. First, a rotation about the z-axis by

$$\rho_i = \frac{\varphi_i}{N}$$

is applied to ensure the correct circumferential tooth spacing. Subsequently, the profile is rotated about the y-axis by $-\varphi_i$ to align it tangentially with the local tool trajectory. Finally, the profile is translated to the position vector

$$\vec{r}_i = \begin{pmatrix} x_i \\ y_i \\ z_i \end{pmatrix} = \begin{pmatrix} r_F \cos\varphi_i \\ 0 \\ r_F \sin\varphi_i \end{pmatrix}.$$

The discretized profile sections are connected by a multi-section sweep operation along the path defined by the sequence of profile center position vectors $\vec{r}_i$. A Frenet-frame-based sweep formulation is employed to ensure a continuous orientation of the profile along the curved trajectory, resulting in a smooth helical cutting edge geometry (Fig. 6b).

From a kinematic perspective, the tool geometry implicitly represents the superposition of two coupled rotational motions: the rotation of the tool around its own axis and the simultaneous rolling motion of the virtual spur gear defined by the profile. A full revolution of the tool along the circular path corresponds to an angular advance of the virtual spur gear by $2\pi/N$, ensuring a generative tooth formation consistent with the hobbing principle.

Numerically, the resulting geometry is implemented as an explicit three-dimensional CAD solid that can be directly employed in Boolean subtraction operations with the face gear blank. Only the functional cutting region is modeled; shank geometry, clearance angles, and chamfers are omitted. The parameterization is intentionally kept compact and includes the module, tool radius r_F, number of teeth N, pressure angle, and profile shift.

This tool model provides a robust and kinematically consistent basis for simulating both idealized machining conditions and systematically introduced tool positioning errors. Based on this representation, the subsequent section describes the modeling of the machining process itself, in which the tool is guided relative to the rotating face gear blank and the resulting geometry is generated by Boolean material removal (Fig. 6c).

4.5 Process Modelling

A key capability of the simulation model is the targeted introduction of manufacturing deviations in order to analyse their influence on the resulting tooth geometry. The model distinguishes between static deviations of the tool position (translational errors) and time-dependent deviations of the motion (wobble errors).

4.5.1 Translational deviations (positioning errors) Translational deviations describe static errors in the initial alignment of the tool relative to the workpiece. These deviations remain unchanged over the entire manufacturing process. The nominal start position of the tool, described by the position vector $\vec{r}_{\text{nominal}}$, is shifted by the translational deviation vector

$$\Delta\vec{r} = (\Delta x, \Delta y, \Delta z)^{\mathsf{T}}.$$

The resulting actual tool position is given by

$$\vec{r}_{\text{real}} = \vec{r}_{\text{nominal}} + \Delta\vec{r}. \tag{6}$$

The effects of the individual deviation components can be summarised as follows:

- **Deviation in x-direction (Δx):** This deviation is the most critical for the present investigation. An offset in the x-direction (tangential to the tool path) causes the tool to engage the tooth space asymmetrically. As a result, one flank is machined more strongly (higher material removal), while the opposite flank is machined less strongly. **The direct consequence is an asymmetric tooth geometry**, which constitutes a central objective of this analysis.
- **Deviation in y-direction (Δy):** A displacement in the y-direction does not introduce a distinct geometric error in the generated face gear geometry. As long as the cutting process spans the complete axial thickness of the face gear, the resulting tooth flanks remain fully generated.
- **Deviation in z-direction (Δz):** An axial shift of the tool leads to a displacement of the tooth profile along the face width. This can alter the location of the contact zone.

4.5.2 Rotational deviation (wobble error) In contrast to static translational deviations, the wobble error is a dynamic disturbance that occurs during tool rotation. It represents, for example, an imbalance or an axial runout of the tool spindle, such that the tool axis is not fixed in space but performs a periodic tilting motion.

The wobble error is characterised by two quantities:

- **Wobble angle (α):** maximum tilt angle of the tool axis during rotation
- **Wobble distance (d):** distance between the tool and the point of rotation

In the transformation, this error is represented by a combination of rotation matrices. The overall rotation consists of a rotation about the x-axis by the angle ϕ, followed by a rotation about the y-axis by the wobble angle α, and a subsequent rotation about the x-axis by ϕ. This composite rotation acts on the offset vector

$$\vec{d} = (d,\, 0,\, 0)^{\mathsf{T}},$$

which represents the wobble distance.

The consequence of the wobble error is a complex periodic variation of the cutting result. Instead of a straight tooth flank, slightly wavy or crowned surfaces can occur. Since the error repeats with every revolution of the tool, it can lead to geometric deviations that are difficult to diagnose and to an uneven load distribution during later gearbox operation.

By deliberately superimposing translational and rotational deviations, the simulation model enables a systematic investigation of how specific machine inaccuracies translate directly into measurable geometric deviations on the final face gear.

Figure 7 summarizes the implemented deviation model, showing the wobble parameters d and α as well as the superimposed translational offset vector $\Delta\vec{r}$, except for the y-component (out of the drawing plane).

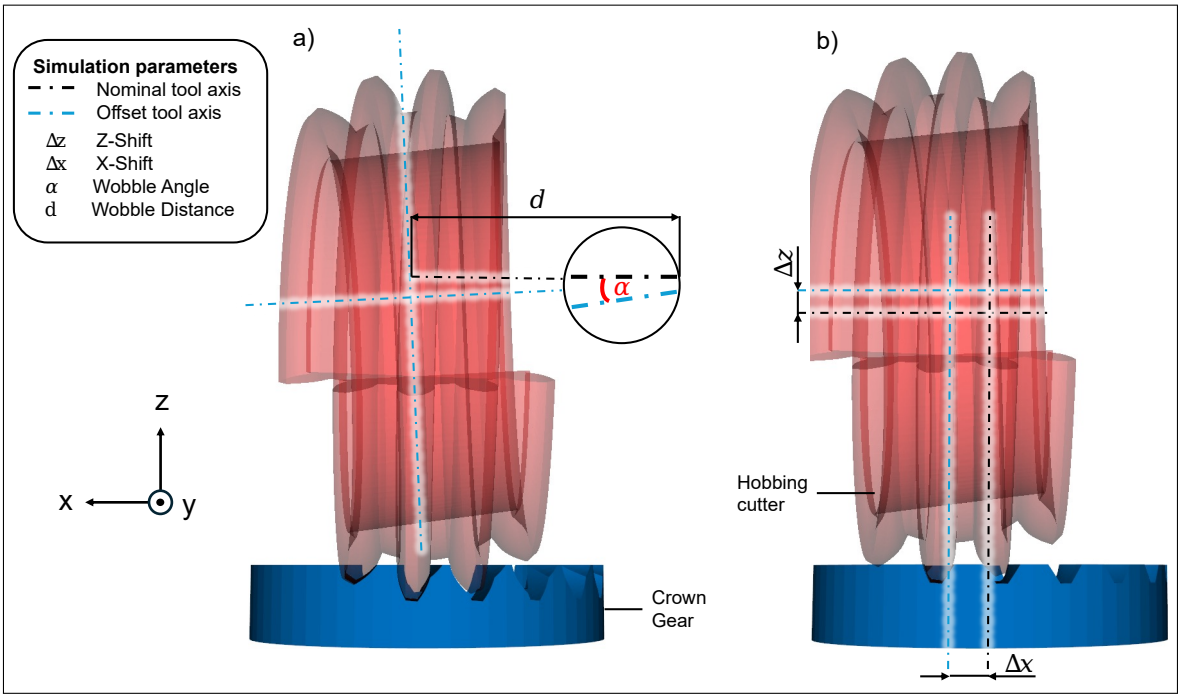

Figure 7: Visualization of the deviation parameters. a) visualizes the wobble distance as well as the wobble angle; b) visualizes the translational errors Δz and Δx

4.5.3 Nominal infeed modelling in y-direction Due to the curved, toroidal geometry of the face gear tool, the complete generation of a tooth flank requires a deterministic infeed motion in y-direction. In the simulation, this infeed is modelled as an incremental y-translation superimposed onto the rotational tool motion.

After each complete revolution of the tool around the face gear, the transformation includes an additional translation Δy_{infeed}, such that the tool is progressively traversed from the outer diameter towards at least the inner diameter. This ensures full radial coverage of the tooth flank.

The resulting nominal infeed must be distinguished from a translational deviation Δy, which represents a static positioning error relative to the nominal infeed path.

4.5.4 Correction of the effective tool helix angle Manufacturing experiments with the developed face gear tool revealed asymmetric tooth shapes. The reason is that the spur-gear profile, modelled as a toroidal winding, is not guided solely along the toroidal path but also exhibits an effective helix angle. This results from the geometry of the profile winding around the toroidal surface, since after a complete 360° rotation of the tool the profile advances by one transverse pitch p_t.

In the current modelling, the tool is generated by a simple wrapping of the spur-gear profile along the torus path. This sweep introduces a geometrically induced helix angle that is not initially considered in the tool orientation. The direct consequence is an asymmetric tooth geometry, expressed by unequal material removal on the two tooth flanks.

To correct this effect systematically, the tool is rotated about its z-axis by a representative mean helix angle α_{mean}. This correction step corresponds to common practice in hobbing, where the tool orientation is adjusted to eliminate the influence of the tool helix on the resulting tooth shape.

The determination of this angle comprises three steps:

1. **Local helix angle:** The local helix angle $\alpha(\varphi)$ is derived as a function of the angular position along the winding and describes the local inclination of the profile.

2. **Mean helix angle:** A representative mean value over one complete winding is defined as

$$\alpha_{\text{mean}} = \arctan\left(\frac{p_t}{L}\right), \tag{7}$$

   where p_t denotes the transverse pitch and L denotes the arc length of one complete winding.

3. **Application of the correction:** The tool model is rotated about the z-axis by the angle α_{mean} during the transformation, thereby compensating the systematic asymmetry induced by the helix of the winding.

With this correction, the symmetry of the tooth geometry is restored and both flanks are machined uniformly. This increases the accuracy of the simulation and reflects real manufacturing practice, where tool orientations are deliberately adjusted to compensate geometrically induced helix errors.

4.5.5 Limitations of the Model The presented approach is purely geometry-based and therefore does not represent a physical hobbing process. The Boolean simulation neglects physical effects such as cutting forces, tool deflection, spindle dynamics, lubrication conditions, heat generation, and tool wear. Likewise, chip formation, material removal mechanisms, and tribological interactions are not modelled. As a result, the simulation predicts geometric consequences of kinematic deviations, but not their process-level origins or energetic feasibility. These general limitations are inherent to the abstraction and motivate the subsequent introduction of a more process-oriented model.

5 Qualitative Analysis of Manufacturing Deviations and Validation

Based on the simulation framework developed in the previous chapters, Chapter 5 conducts a qualitative analysis of manufacturing deviations and their effects on face gear geometry. The focus lies on two categories of errors: static translational offsets and dynamic wobble (tumble) effects. Each deviation is first examined in simulation to understand its geometric manifestation on the tooth flanks, and subsequently validated on physical workpieces that were manufactured with the same intentional parameter variations. The real parts were measured using an Alicona μCMM, enabling a direct comparison between simulated predictions and actual geometric outcomes.

5.1 Influence of Translational Offsets

Translational offsets Δx, Δy, and Δz represent static positioning errors of the tool relative to the workpiece. In this analysis, the offset in the feed direction (Δy) is neglected, as it merely shifts the timing of the tool engagement without altering the fundamental flank geometry. Thus, the focus lies on tangential (Δx) and radial/vertical (Δz) deviations.

5.1.1 Tangential Offset The tangential offset Δx proves to be the most critical parameter regarding tooth symmetry.

Kinematic Effect & Simulation As the tool is shifted along the tangent of its rolling path, the kinematic engagement becomes unbalanced. The simulation shows an asymmetric distribution of the functional flank area: the side towards which the tool is shifted exhibits an increased surface area, while the opposing flank suffers from a significant undercut. This results in a "leaned" tooth profile and a systematic pressure angle deviation.

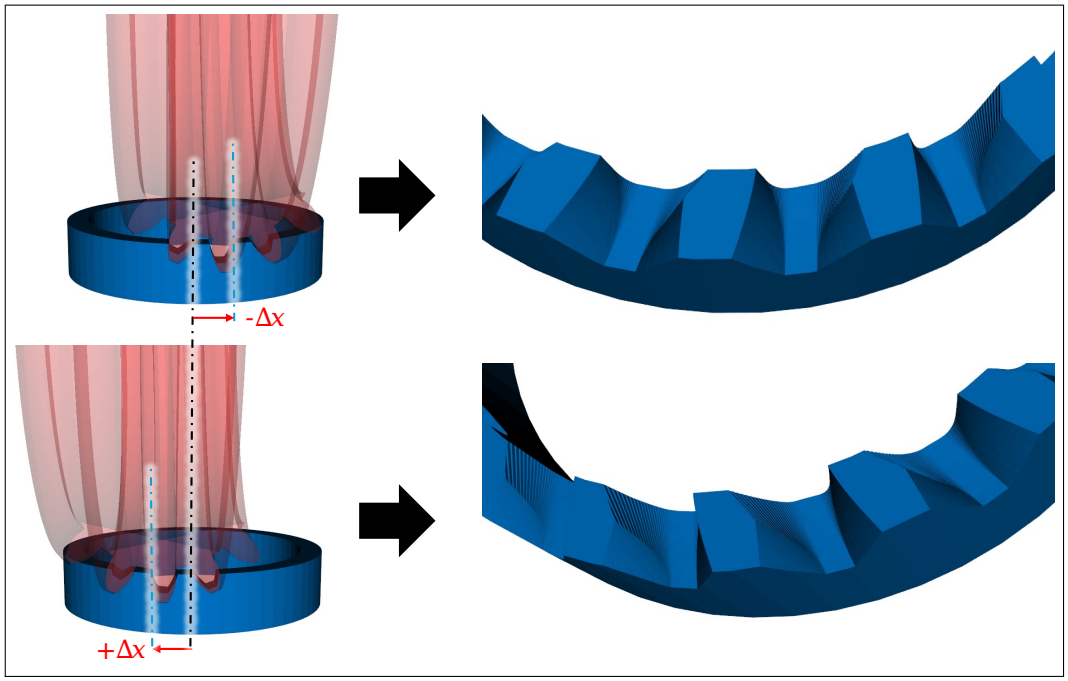

Figure 8: Simulated effect of X-shift: Asymmetric flank formation and localized undercut.

Experimental Validation As previously discussed, a shift of the tool in positive x-direction increases the material engagement on the shifted side. This effect is confirmed in the measurements: on the side towards which the tool was displaced, the functional flank region grows, indicating a wider and more actively load-bearing contact zone. Conversely, on the opposite side, the functional region decreases noticeably. Here, the undercut progresses further into the tooth space and reduces the usable contact area, leading to a diminished flank portion available for load transmission.

This asymmetric change in usable geometry is clearly observable in Figure 9. The geometry on the left (shift $+0.1\,\mathrm{mm}$) exhibits an expanded functional zone, while the geometry on the right (shift $-0.1\,\mathrm{mm}$) shows an increased undercut and a corresponding reduction of the functional region. These results confirm the simulated behavior.

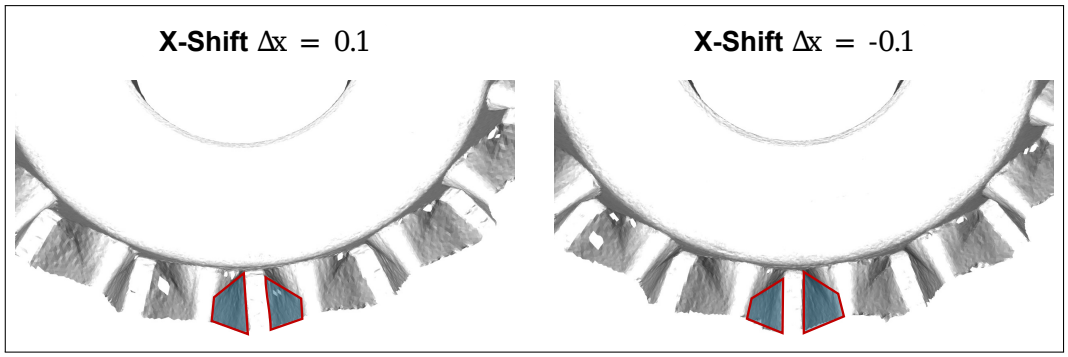

Figure 9: Comparison of measured tooth profiles for a tangential tool offset. The left profile shows a shift of $+0.1\,\mathrm{mm}$ (positive x-direction), the right profile $-0.1\,\mathrm{mm}$ (negative x-direction).

5.1.2 Vertical Offset The offset Δz defines the penetration depth of the tool into the workpiece material.

Kinematic Effect & Simulation The simulation indicates that an increase in Δz leads to a proportional increase in tooth height. This significantly alters the tooth tip geometry: the teeth become increasingly "pointed" (*pointed teeth*), and the width of the top land decreases. Conversely, insufficient depth results in incomplete tooth formation and a reduced contact ratio.

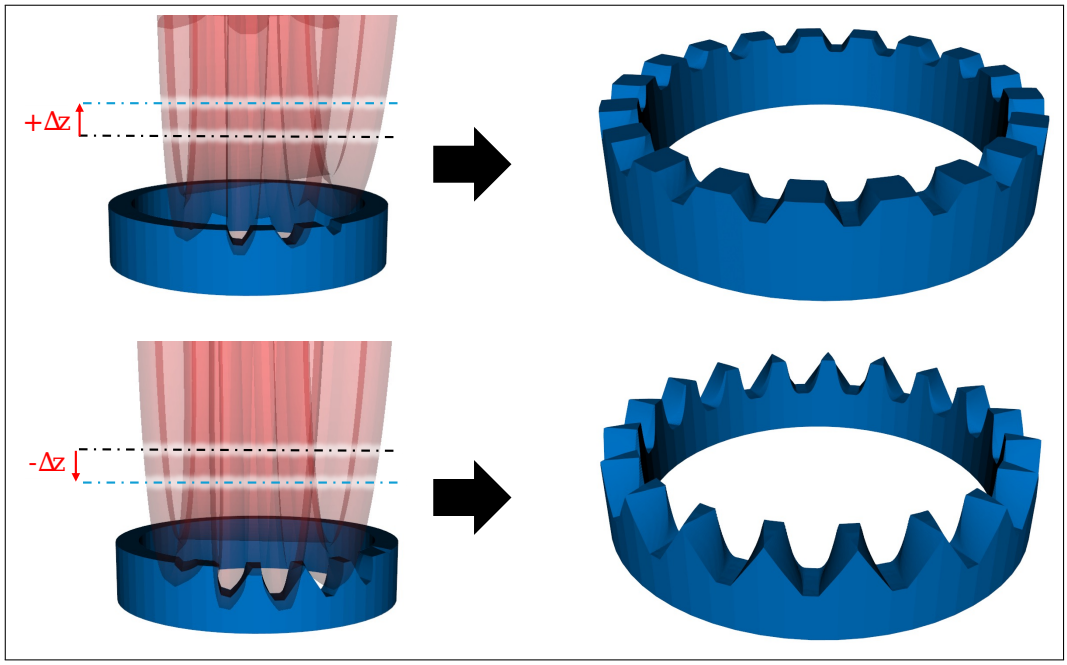

Figure 10: Simulated effect of z-shift: Variation of tooth height and top land thickness.

Experimental Validation The validation with real parts confirms that the vertical position directly controls the radial tooth profile. The measured specimens show that excessive depth leads to a critical reduction in top land thickness, which may fall below safety limits for tooth strength.

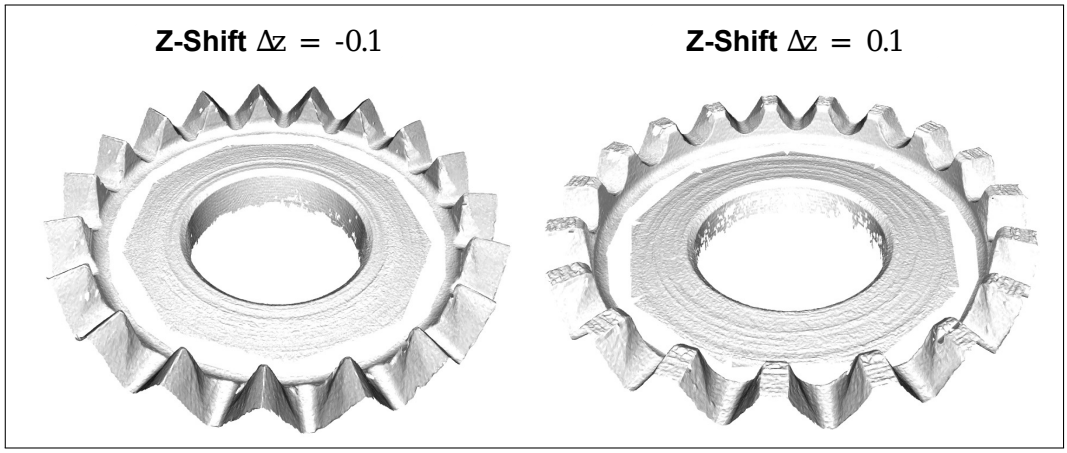

Figure 11: Experimental validation of z-shift: Measured deviation in tooth height and profile curvature.

5.2 Influence of Dynamic Wobble Errors

In contrast to static offsets, the wobble error (tumble) introduces a time-dependent deviation that varies periodically with the rotation angle ϕ.

Kinematic Effect & Simulation The wobble distance (d) and angle (α) define an eccentric and tilted tool rotation. This motion results in multiple overlapping cutting surfaces. The simulation reveals that the most severe damage occurs at the point of maximum eccentricity, where the tool leaves a characteristic "gouge" or scar in the flank. The result is a "hollow" or "fat" tooth form depending on the phase of the wobble.

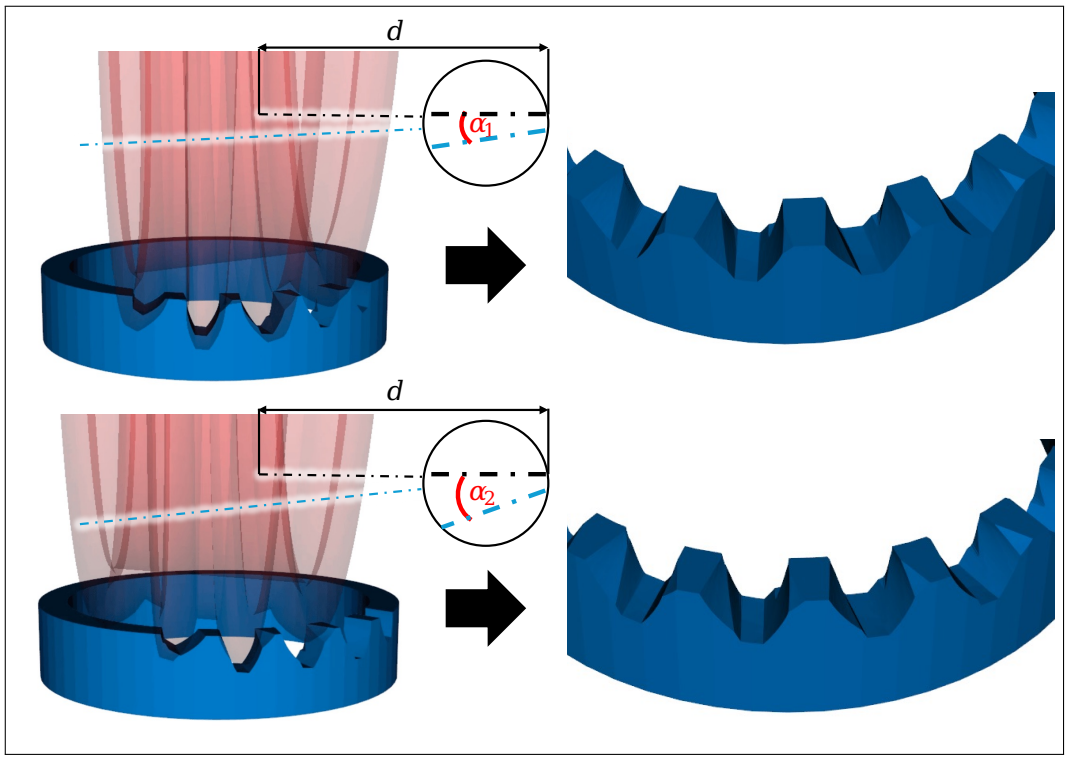

Figure 12: Simulated wobble error: Dynamic surface scarring and periodic flank deviations. With $alpha_2 > alpha_1$ the scarring effects increase.

Experimental Validation The comparison with manufactured parts confirms that the simulated wobble effect qualitatively manifests in the real geometry. While the characteristic periodic scarring predicted by the model does not appear in this magnitude — likely because the required wobble amplitude would exceed the machine's practical limits — the measured flank topographies still show an increased number of facets as well as a more pronounced angular segmentation of the surface. These effects are consistent with the model behaviour and indicate that tool tumble influences the resulting geometry even at low amplitudes.

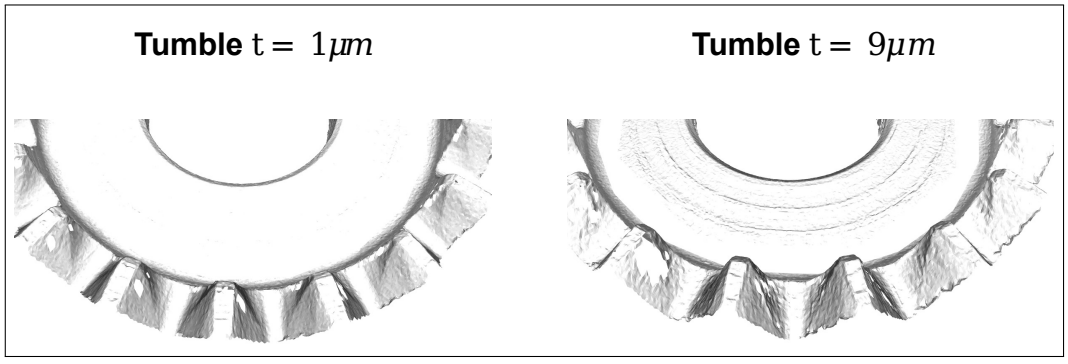

Figure 13: Experimental validation of the tumble effect: Measured flank geometry showing increased faceting and angular segmentation consistent with low-amplitude wobble.

Summary of Findings
The qualitative study demonstrates that the simulation model accurately reproduces characteristic manufacturing errors. The high sensitivity to Δx emphasizes the need for precise centering, while the Δz and wobble analysis provide diagnostic patterns to identify vertical misalignments and spindle inaccuracies in the production process.

6 Conclusion

This paper presented a modular, kinematically driven simulation model for the virtual generation of face gear geometries. The Boolean-based modeling approach separates the ideal target geometry from

manufacturing-related influences, enabling a structured analysis of how specific process parameters translate into geometric deviations on the tooth flanks.

A dedicated tool model based on a toroidal winding of an involute spur gear profile provides the foundation for virtual manufacturing. The model reproduces characteristic geometric features of face gears while maintaining full control over kinematic and positional parameters. Central to this is the helix angle correction, which proved essential for generating symmetrical teeth; without it, the tool's winding geometry introduces systematic asymmetries that obscure the influence of actual manufacturing deviations.

The qualitative sensitivity analysis identified the tangential offset Δx as the most critical positioning parameter, as even small deviations lead to noticeable flank asymmetry. In contrast, the model showed a comparatively low sensitivity to radial displacement. Beyond static errors, the integration of wobble parameters (α, d) allows the simulation of dynamic deviations and their characteristic impact on surface formation.

Overall, the simulation environment provides a structured framework to investigate how machine inaccuracies propagate into geometric gear defects. It supports tolerance definition based on geometric causality rather than empirical heuristics and thus offers a foundation for more systematic manufacturing analysis.

Outlook and Future Work

Future work will include quantitative validation using high-resolution measurements of manufactured parts, as well as extensions toward tool wear, elastic effects, and contact behavior. These additions aim to narrow the gap between idealized kinematic models and real production conditions and to strengthen the link between geometric deviations and functional gear performance.

In another work by Bilen et al. [1], a set of interpretable quality features for face gears has been developed to quantify deviation patterns. Integrating such feature sets into the simulation framework would enable more targeted studies of specific error mechanisms and facilitate the derivation of analytical correction models. This opens additional research pathways towards a deeper causal understanding of process–geometry relationships and ultimately towards simulation-supported manufacturing optimization.

Acknowledgments

The authors would like to sincerely thank Robert Schmitt, Jochen Wacker, and Christoph Rettig from Dentsply Sirona for their valuable support of this work and for contributing their professional expertise throughout the course of the research. Furthermore, the authors gratefully acknowledge Edouard Gindin and Philip Jukl from Frenco GmbH for their support and for sharing their expert knowledge, which significantly contributed to this study.

Data availability

The underlying component data supporting the findings of this study are confidential due to industrial cooperation agreements and therefore cannot be made publicly available.

References

[1] Ali Bilen et al. "Quality Features for Holistic Evaluation and Quality Control of Micro Face Gears". In: *Measurement: Sensors* (2025). In Review.

[2] DIN 868. *DIN 868:1976-12 – allgemeine begriffe und bestimmungsgrößen für zahnräder, zahnradpaare und zahnradgetriebe*. Deutsche Norm. Berlin, Germany, Dec. 1976. URL: https://www.dinmedia.de/din-normen/1077532.

[3] esco GmbH engineering solutions consulting. *PTM 3-6-4-0, Build 23971: Precision-Tool Manufacturing*. Published: Technical product documentation. 2020.

[4] Edouard Gindin, Ali Bilen, and Gisela Lanza. "Eine mathematische beschreibung der flankengeometrie geradverzahnter Kronenräder". In: *tm - Technisches Messen* (2025). Publisher: De Gruyter. ISSN: 0171-8096, 2196-7113. DOI: 10.1515/teme-2025-0033.

[5] Claude Gosselin. *HyGEARS Updates: Build 500.00 (04 October 2021) and Build 500.10 (09 January 2023)*. Quebec, Canada: Involute Simulation Softwares Inc., 2021. URL: https://www.hygears.com.

[6] Jonas-Frederick Hochrein et al. "Direct flank geometry calculation for face gears". In: *Forschung im Ingenieurwesen* 86.3 (Jan. 2022), pp. 617–625.

[7] KISSsoftAG. *Kronenräder: Geometrie und Festigkeit - KISSsoft AG*. Ed. by yumpu.com. Jan. 2012.

[8] Fritz Klocke and Christian Brecher. *Zahnrad- und Getriebetechnik: Auslegung – Herstellung – Untersuchung – Simulation*. Hanser eLibrary. München: Carl Hanser Verlag, Jan. 2017. ISBN: 978-3-446-43140-9. DOI: 10.3139/9783446431409. URL: http://www.hanser-elibrary.com/doi/book/10.3139/9783446431409.

[9] Chao Lin et al. "Pitch deviation measurement and analysis of curve-face gear pair". In: *Measurement* 81 (Jan. 2016), pp. 95–101. ISSN: 0263-2241.

[10] F. L. Litvin and A. Fuentes. *Gear Geometry and Applied Theory*. 2nd. New York: Cambridge University Press, Jan. 2011.

[11] F. L. Litvin et al. "Design and Geometry of Face-Gear Drives". en. In: *Journal of Mechanical Design* 114.4 (Dec. 1992), pp. 642–647. ISSN: 1050-0472, 1528-9001. DOI: 10.1115/1.2917055. URL: https://asmedigitalcollection.asme.org/mechanicaldesign/article/114/4/642/454144/Design-and-Geometry-of-FaceGear-Drives (visited on 03/21/2025).

[12] Faydor L. Litvin et al. "Face-gear drive with spur involute pinion: geometry, generation by a worm, stress analysis". In: *Computer Methods in Applied Mechanics and Engineering* 191.25 (Jan. 2002), pp. 2785–2813. ISSN: 0045-7825.

[13] Faydor L. Litvin et al. *Handbook on face gear drives with a spur involute pinion*. Tech. rep. Jan. 2000.

[14] Xinxin Lu et al. "A measurement solution of face gears with 3d optical scanning". In: *Materials* 15.17 (Jan. 2022). Publisher: MDPI, p. 6069.

[15] Xinxin Lu et al. "A novel mathematical model for the accurate measurement of face gears by considering the geometric deviations of multiple teeth". In: *Measurement* 231 (Jan. 2024), p. 114545. ISSN: 0263-2241.

[16] Karlheinz Roth. *Zahnradtechnik Evolventen-Sonderverzahnungen zur Getriebeverbesserung: Evoloid-, Komplement-, Keilschräg-, Konische-, Konus-, Kronenrad-, Torus-, Wälzkolbenverzahnungen, Zahnrad-Erzeugungsverfahren*. Vol. 3. Springer-Verlag, Jan. 2013.

[17] Jinyang Tao et al. "An efficient and accurate measurement method of tooth flank variations for face gears". In: *Measurement* 221 (Jan. 2023), p. 113486. ISSN: 0263-2241.

[18] VDI 2731 Blatt 1. *VDI 2731 Blatt 1:2009-04 – Mikrogetriebe– Grundlagen*. Tech. rep. Düsseldorf: Verein Deutscher Ingenieure (VDI), 2009. URL: https://www.vdi.de/richtlinien/details/vdi-2731-blatt-1-mikrogetriebe-grundlagen.

[19] Shenghui Wang et al. "Digital tooth contact analysis of face gear drives with an accurate measurement model of face gear tooth surface inspected by CMMs". In: *Mechanism and Machine Theory* 167 (Jan. 2022), p. 104498. ISSN: 0094-114X. DOI: 10.1016/j.mechmachtheory.2021.104498. URL: https://www.sciencedirect.com/science/article/pii/S0094114X2100255X (visited on 11/28/2025).

[20] Yanzhong Wang et al. "A hobbing method for spur face gears with bidirectional modification". In: *The International Journal of Advanced Manufacturing Technology* (Jan. 2022). Publisher: Springer, p. 112. ISSN: 0268-3768.